Electronic Supplementary Material (ESI) for RSC Advances

Supporting Information

The Thermofluoric Behavior of Poly(fluorenetolyldiphenylamine)-Oxadiazole Pair in Polymer Matrix.

Chin-Sheng Lee,[†] Cheng-Po Kuo,[†] Chiou-Ling Chang,[†] Ching-Nan Chuang,[‡] Mandy M. Lee,[#] Shih-Sheng Sun,[#] and Man-kit Leung*[,†,‡]

**Correspondence to: Man-kit Leung (E-mail: mkleung@ntu.edu.tw)*

[†] *Department of Chemistry, National Taiwan University, 1 Roosevelt Road Section 4, Taipei, Taiwan 10617, ROC.* [‡] *Institute of Polymer Science and Engineering, National Taiwan University.* [#] *Institute of Chemistry, Academia Sinica, Nankang, Taipei 115, Taiwan, ROC.*

Contents of Supporting Information.....S1

Supporting Figure S1. ^{1}H NMR Spectrum of **1**

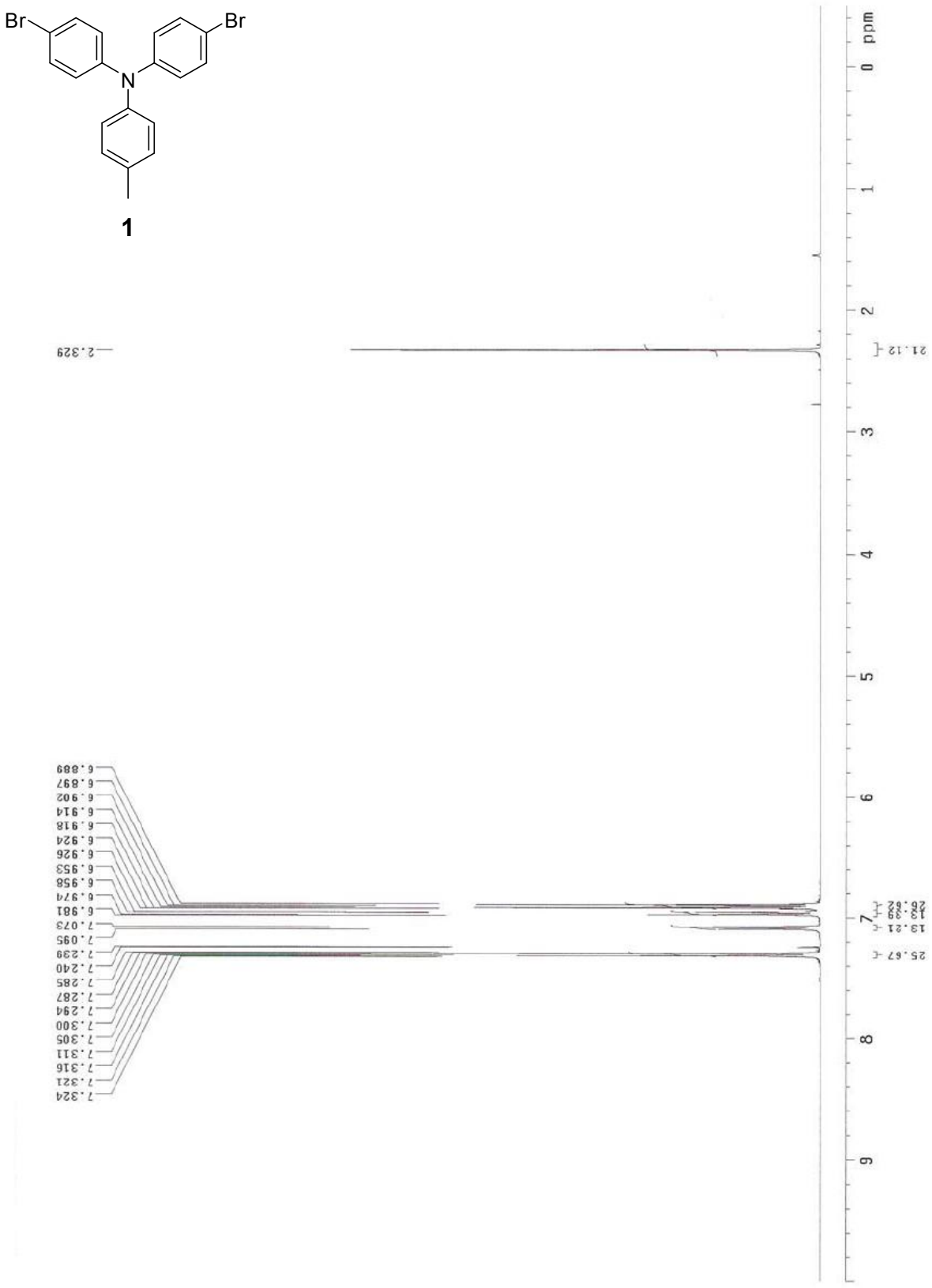

Supporting Figure S2. ^{13}C NMR Spectrum of **1**

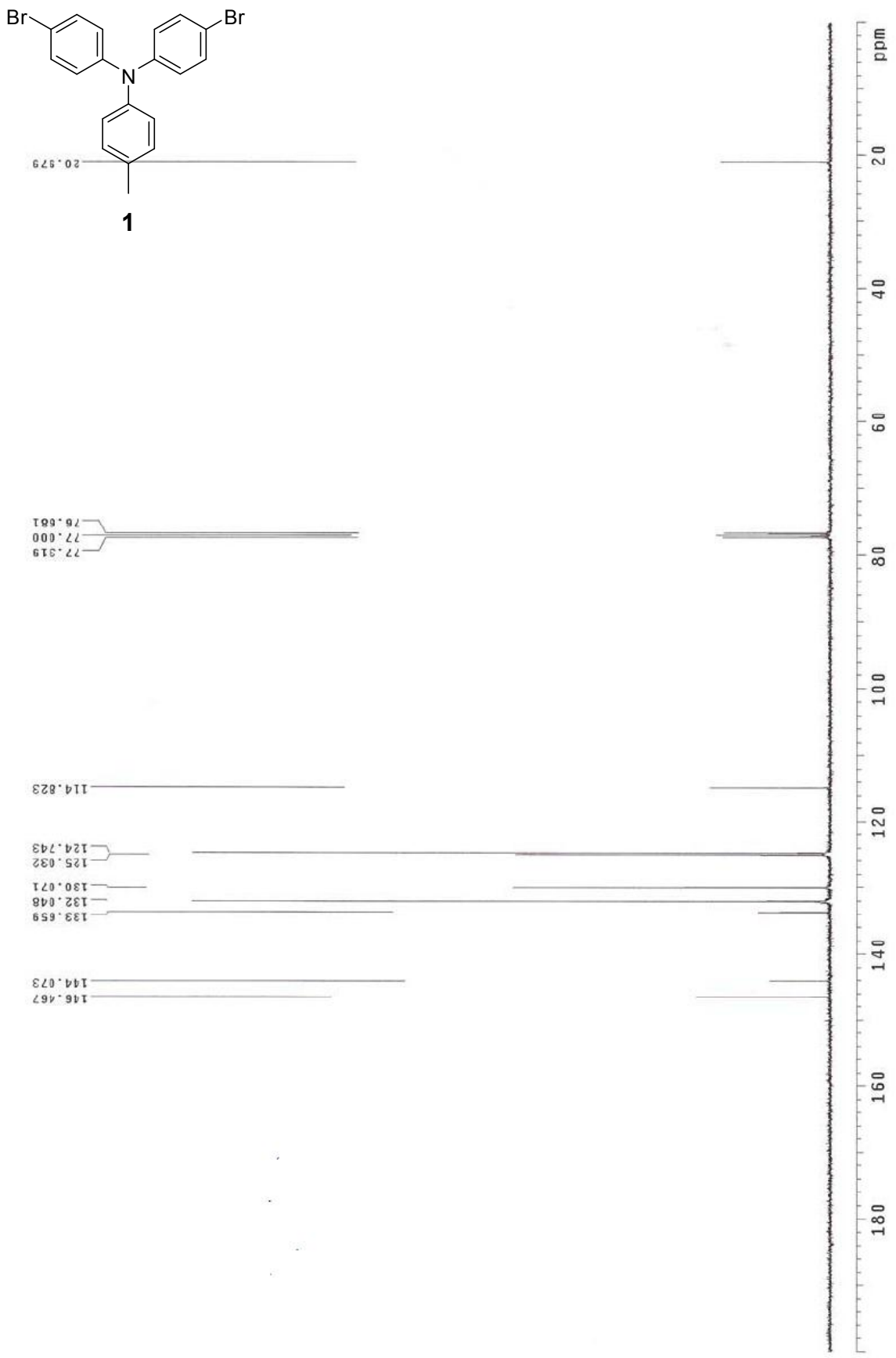

Supporting Figure S3. ^{1}H NMR Spectrum of **2**

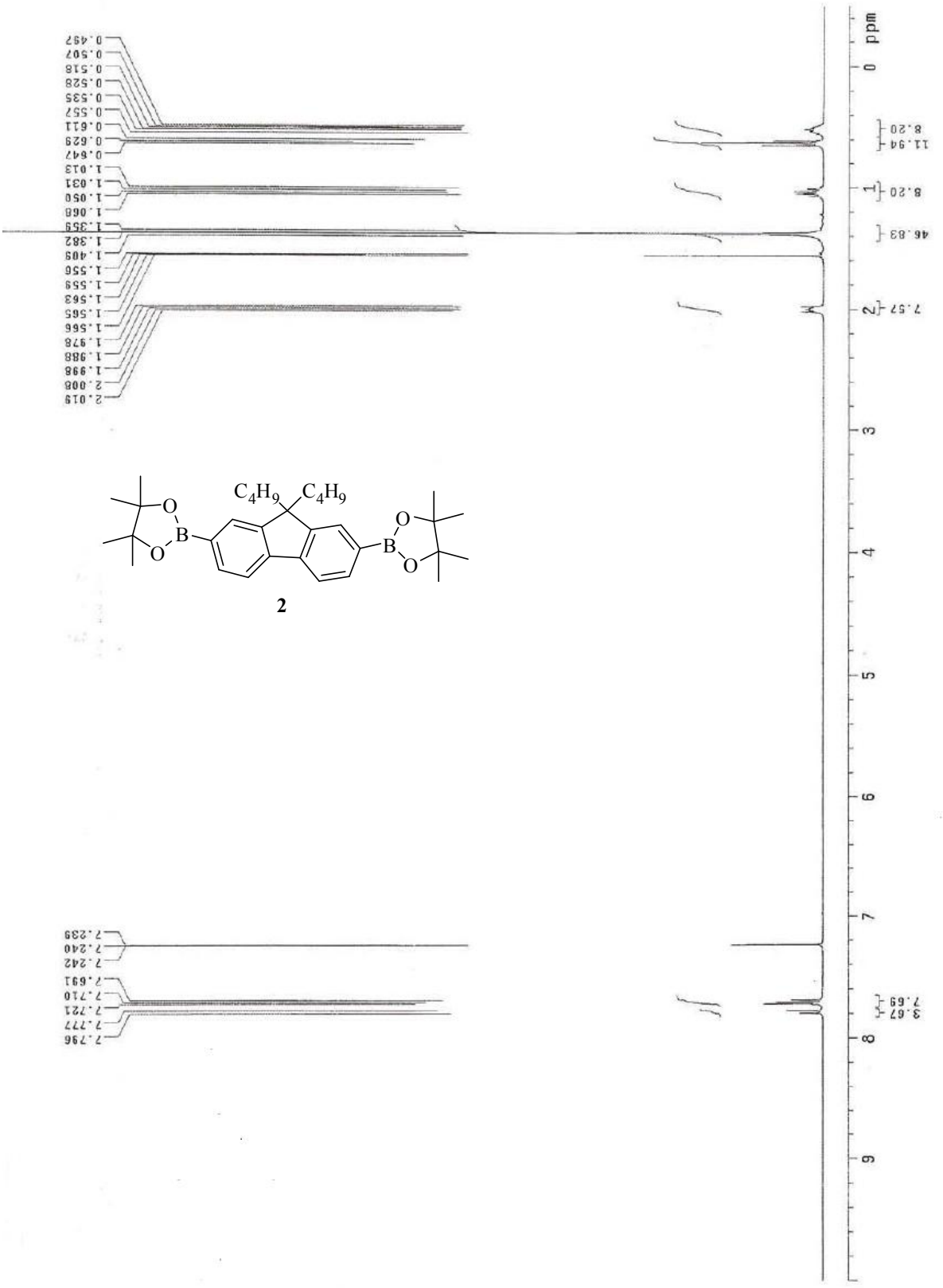

2

Supporting Figure S4. ^{13}C NMR Spectrum of **2**

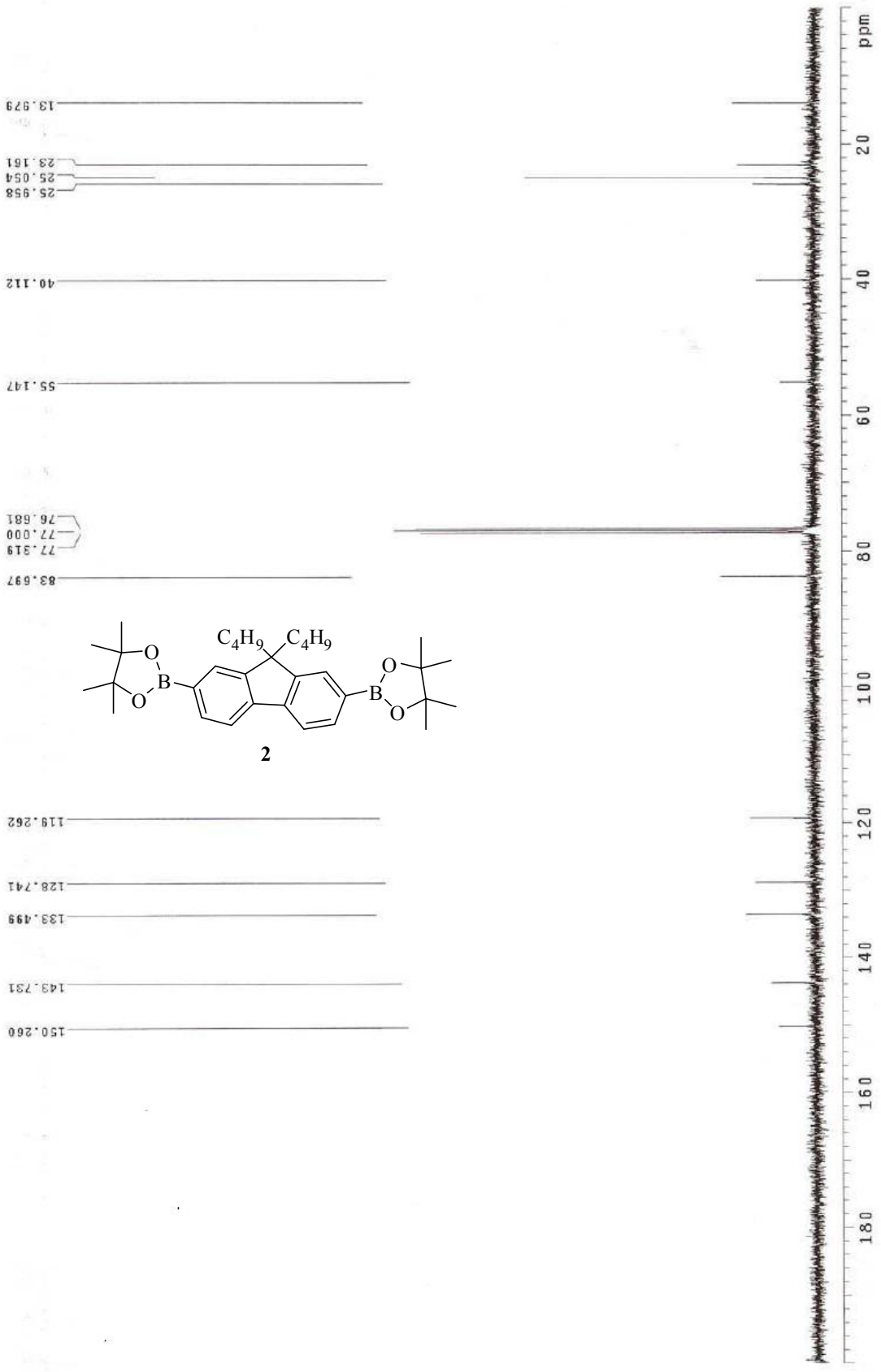

2

Supporting Figure S5. ^{1}H NMR Spectrum of **PFT**

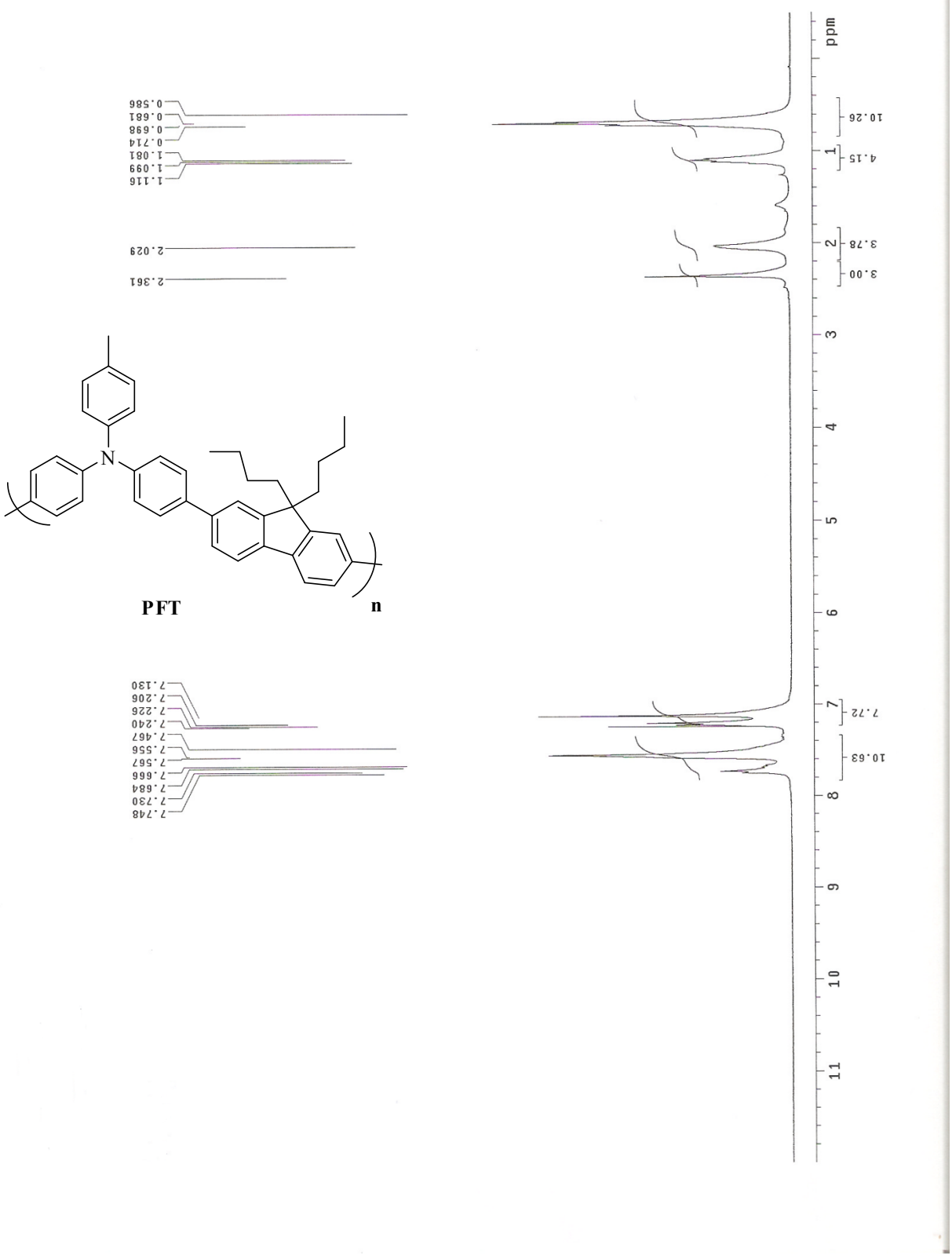

Supporting Figure S6. ^{1}H NMR Spectrum of **3**

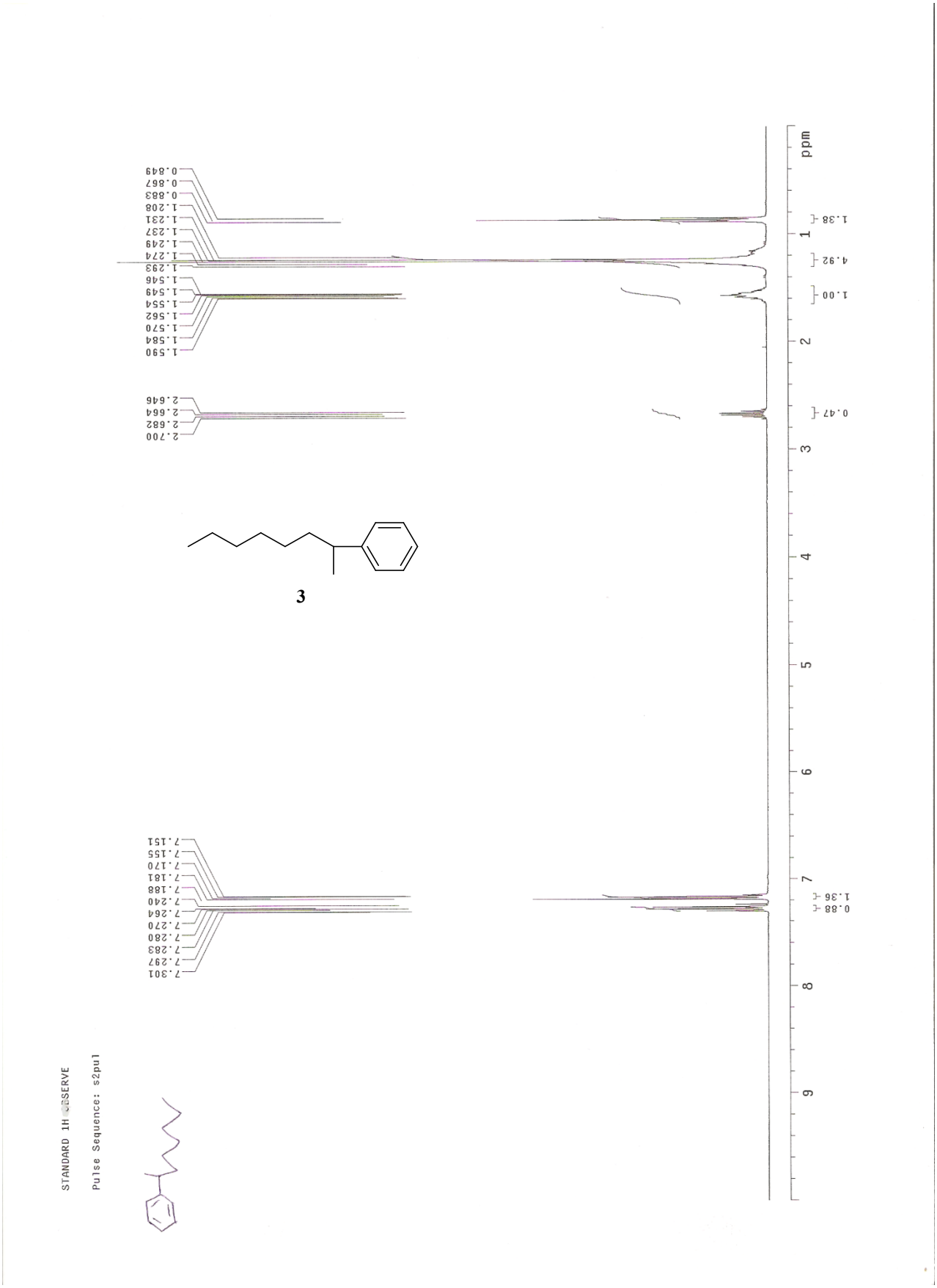

3

Supporting Figure S7. ^{13}C NMR Spectrum of **3**

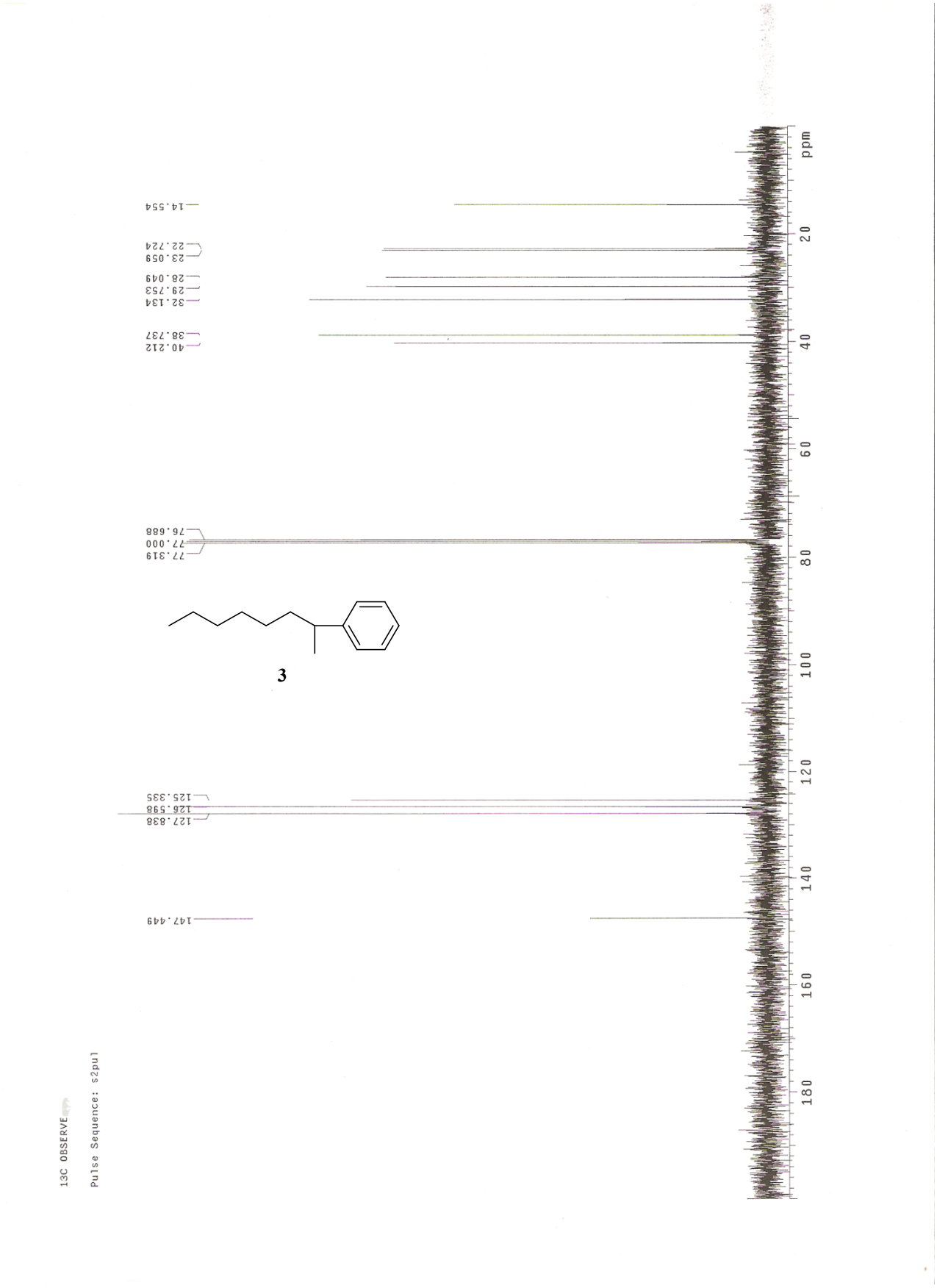

3

Supporting Figure S8. ^{1}H NMR Spectrum of **4**

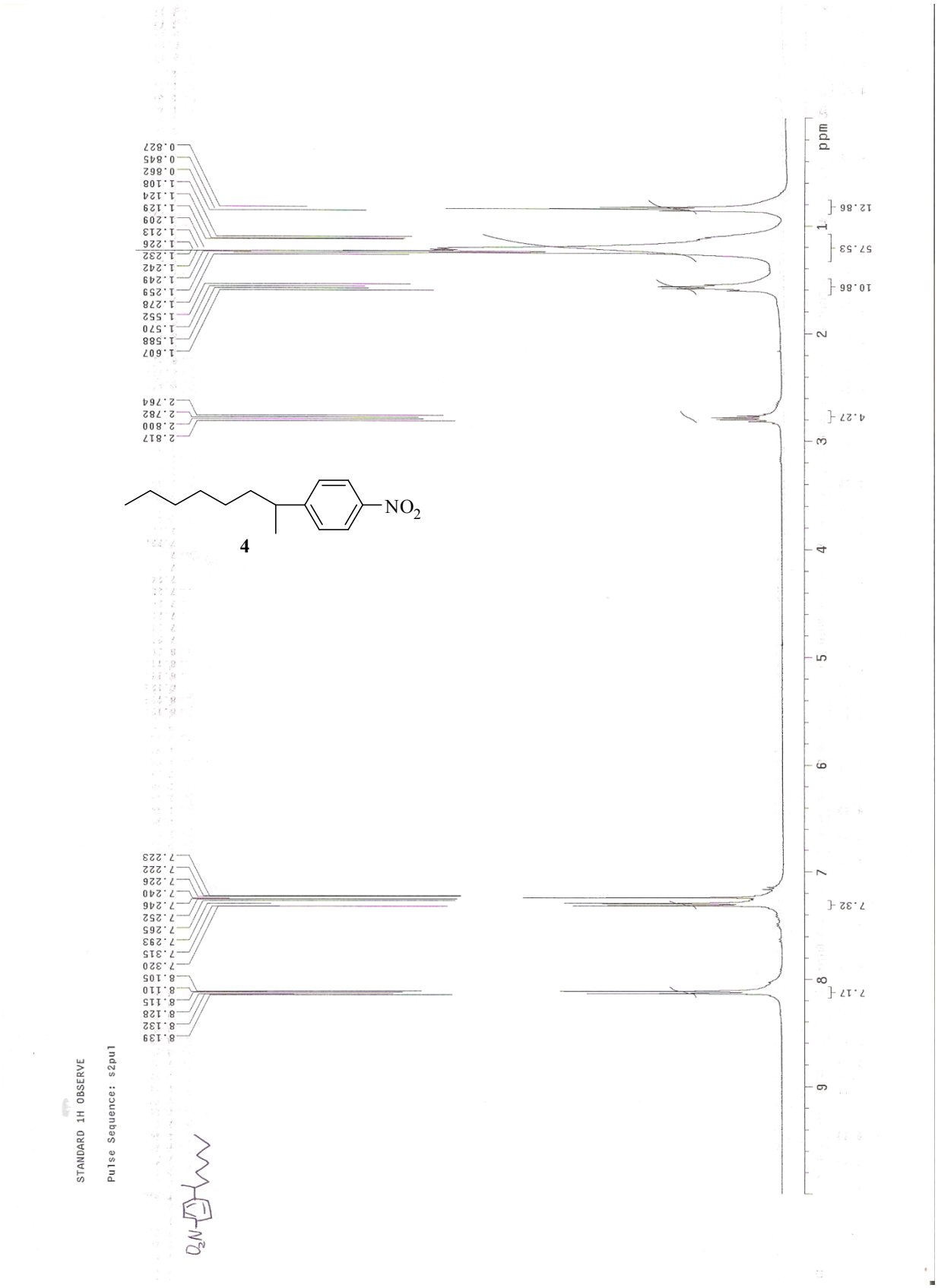

Supporting Figure S9. ^{13}C NMR Spectrum of **4**

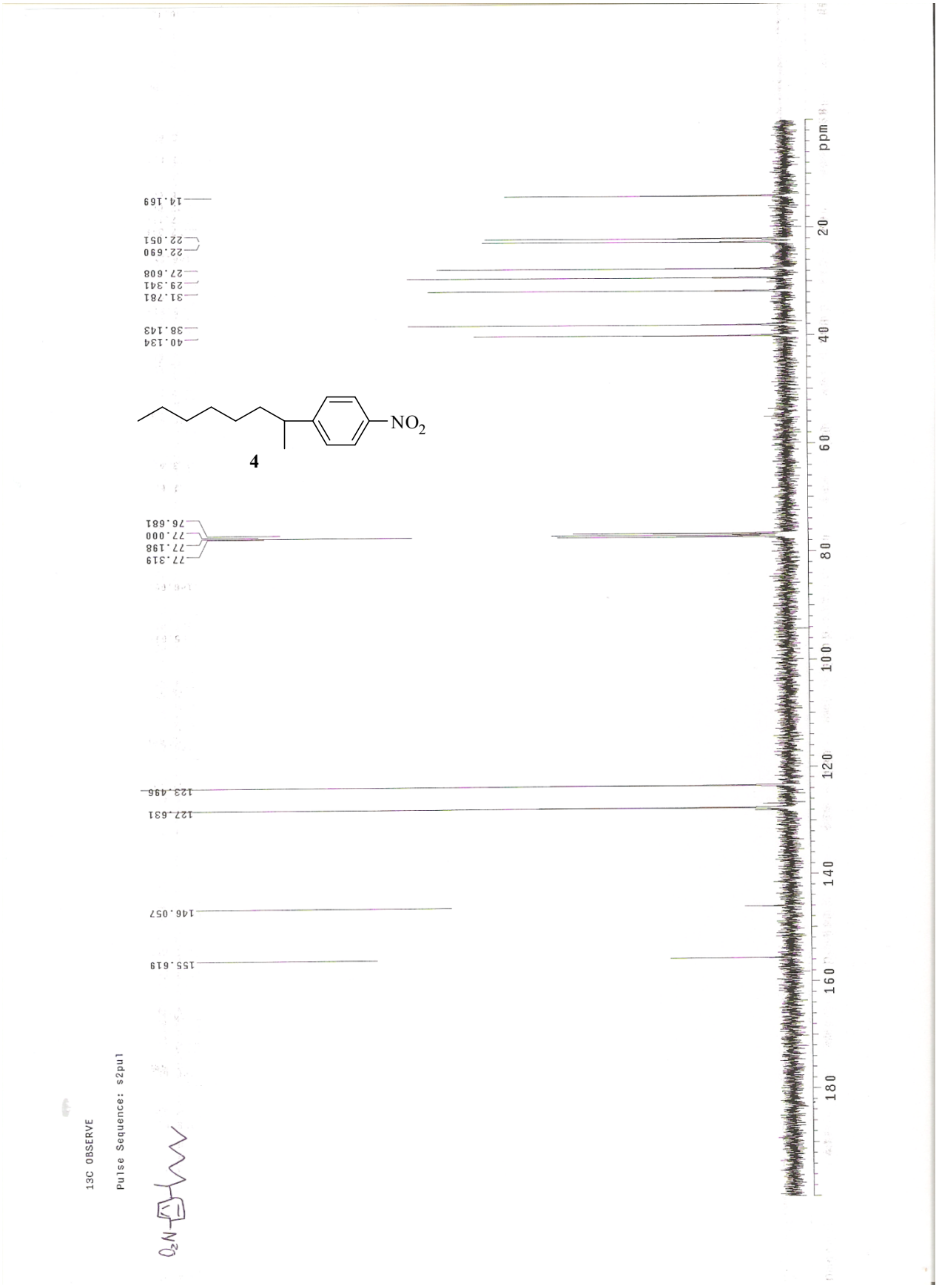

Supporting Figure S10. ^{1}H NMR Spectrum of **5**

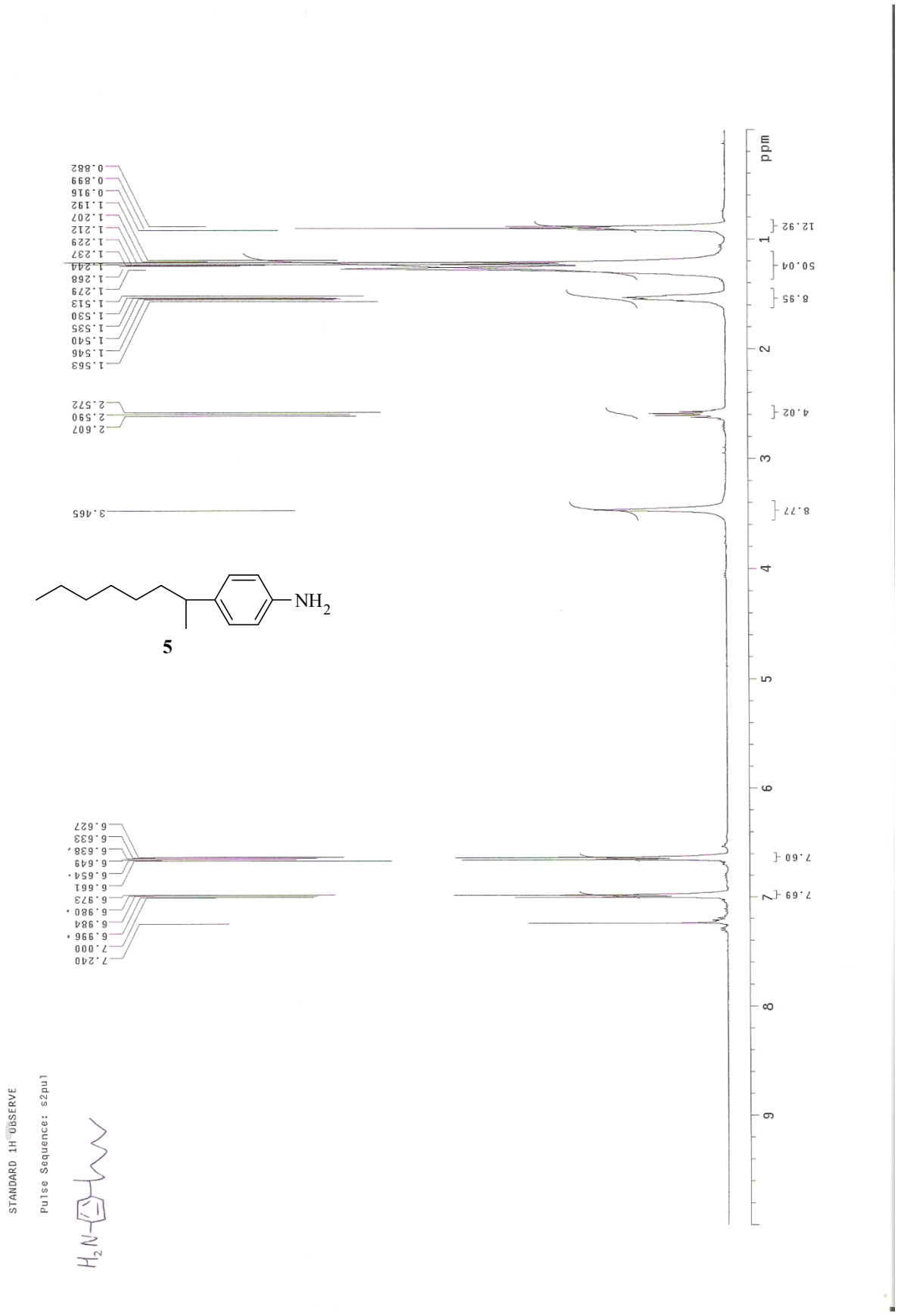

Supporting Figure S11. ^{13}C NMR Spectrum of **5**

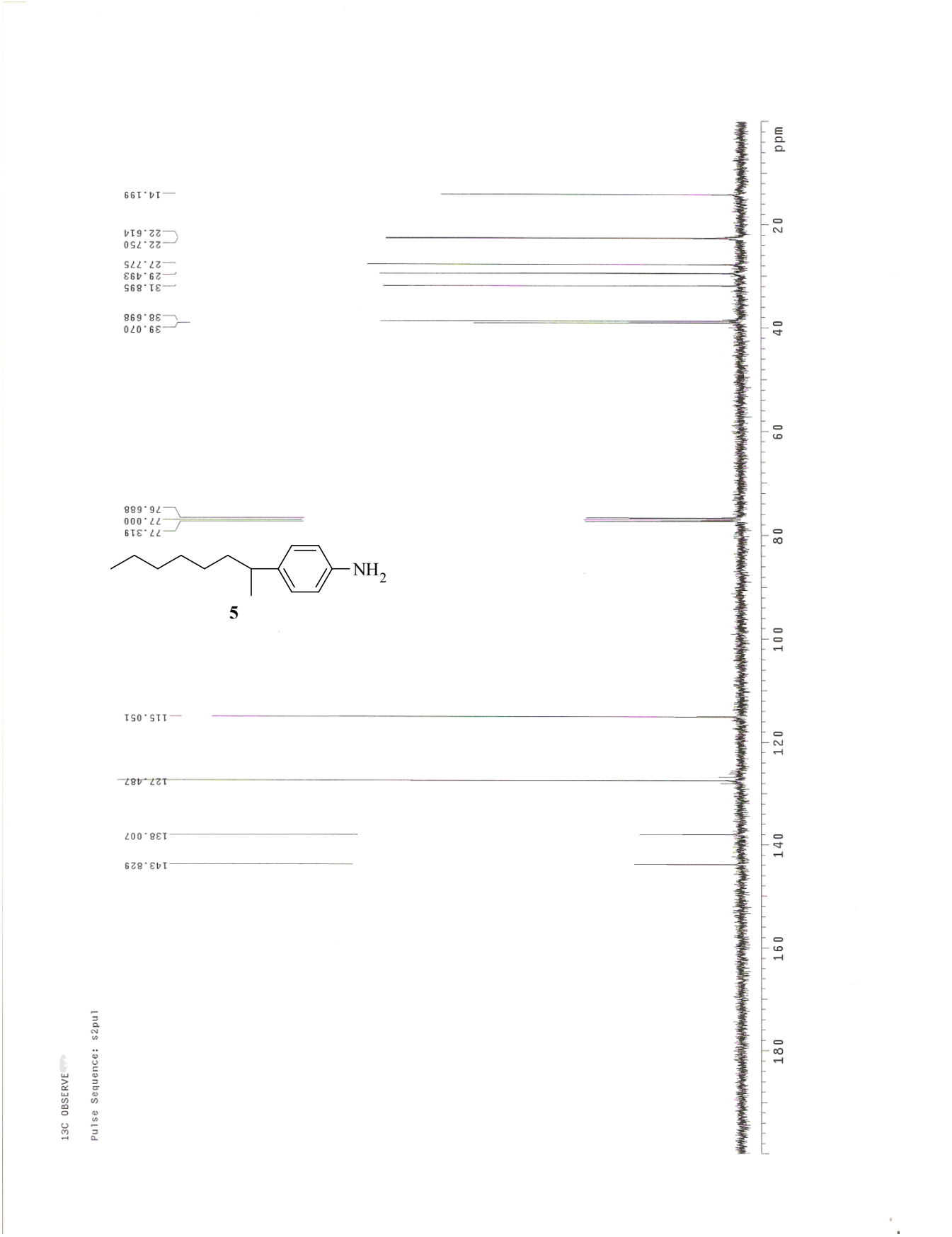

Supporting Figure S12. ^{1}H NMR Spectrum of **6**

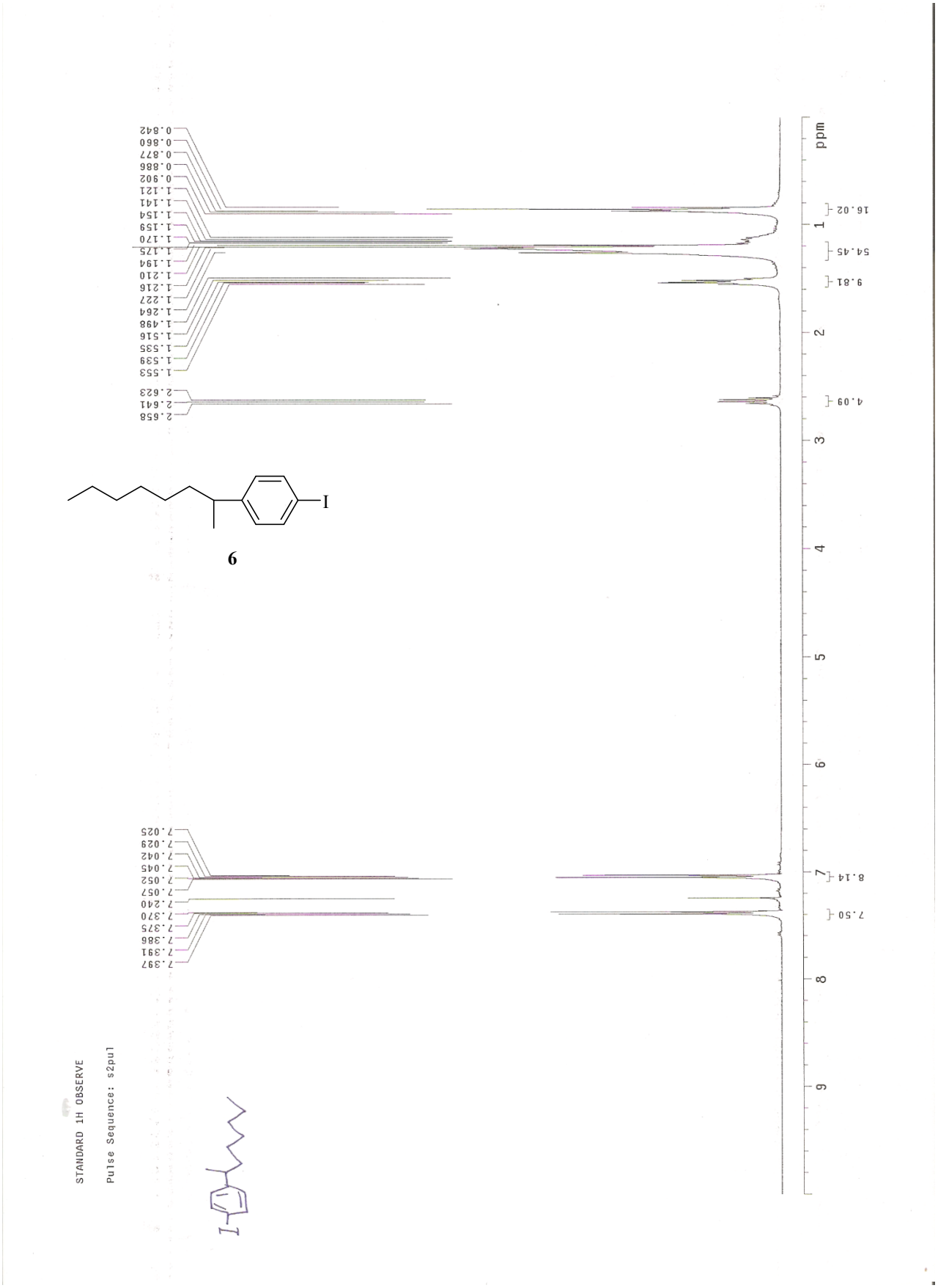

Supporting Figure S13. ^{13}C NMR Spectrum of **6**

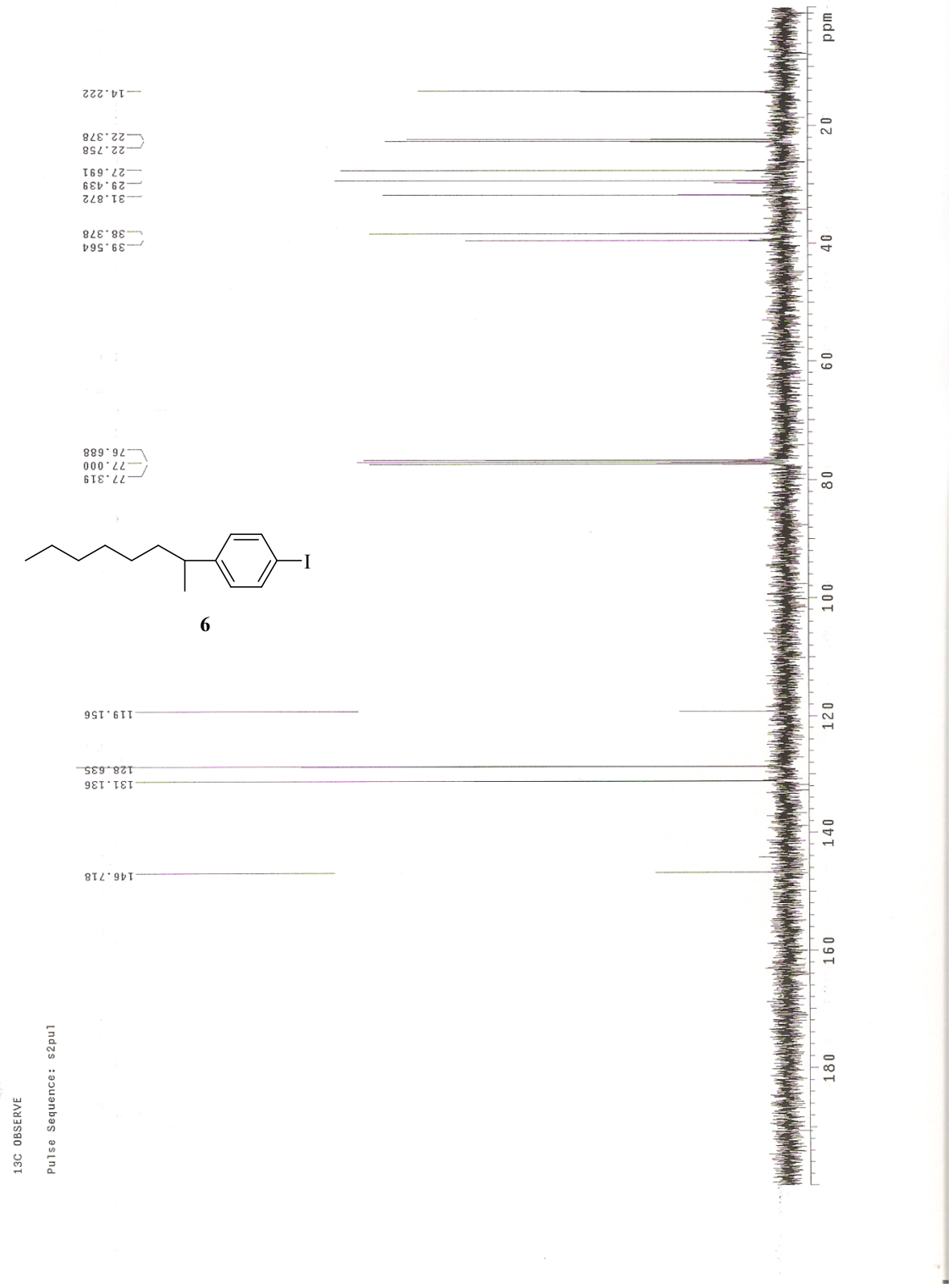

Supporting Figure S14. ^{1}H NMR Spectrum of **7**

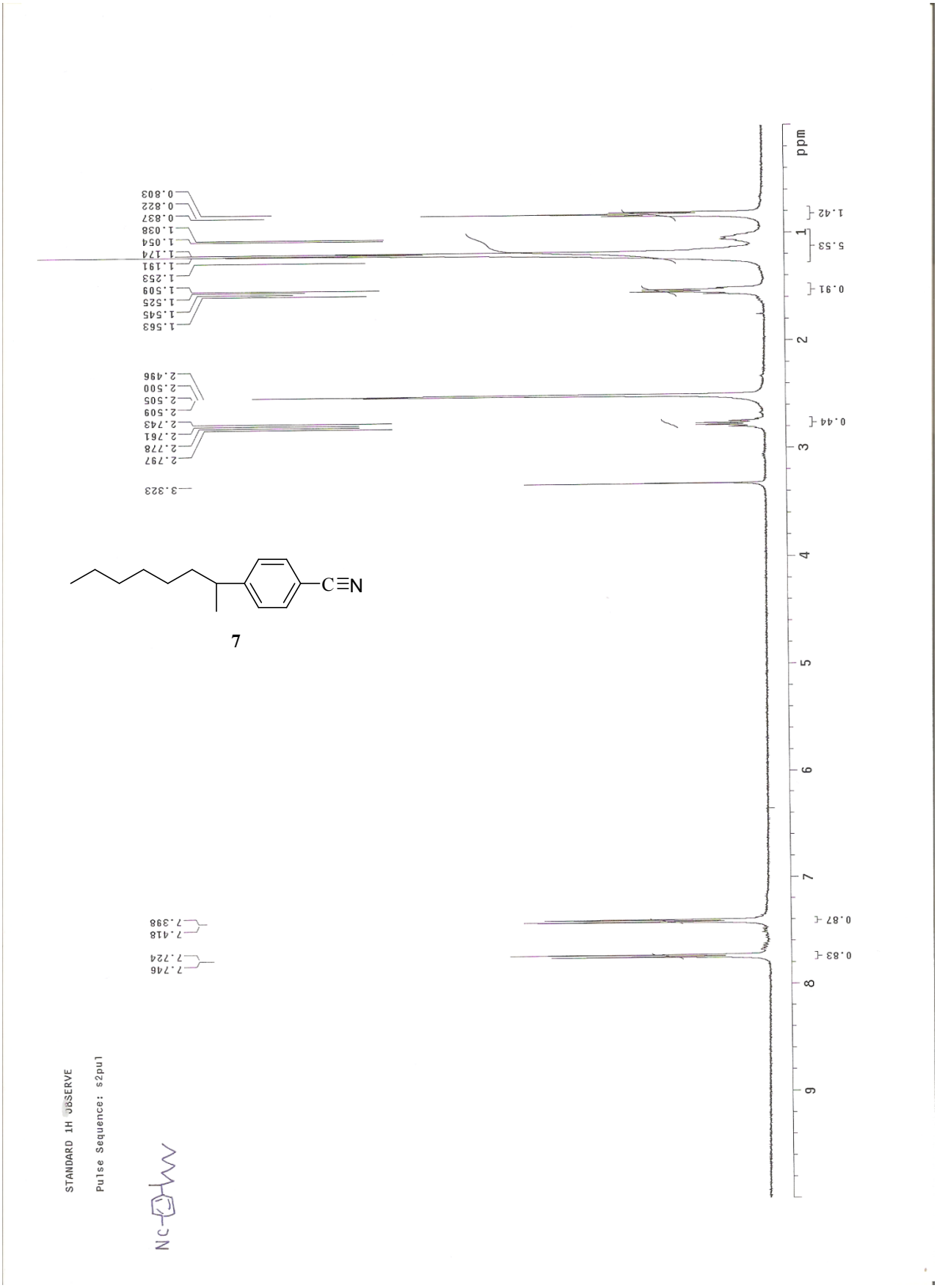

Supporting Figure S15. ^{13}C NMR Spectrum of **7**

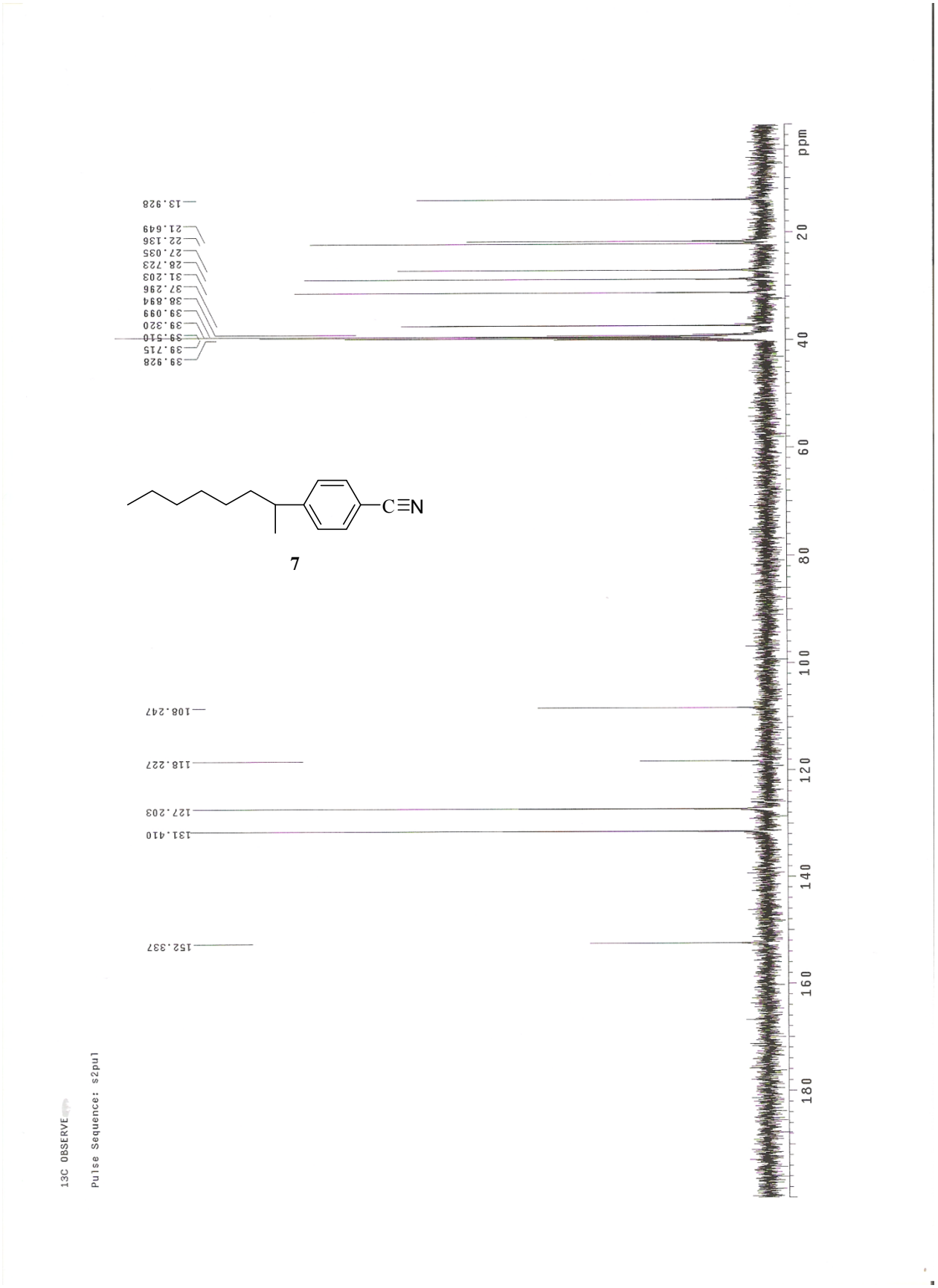

Supporting Figure S16. ^{1}H NMR Spectrum of **8**

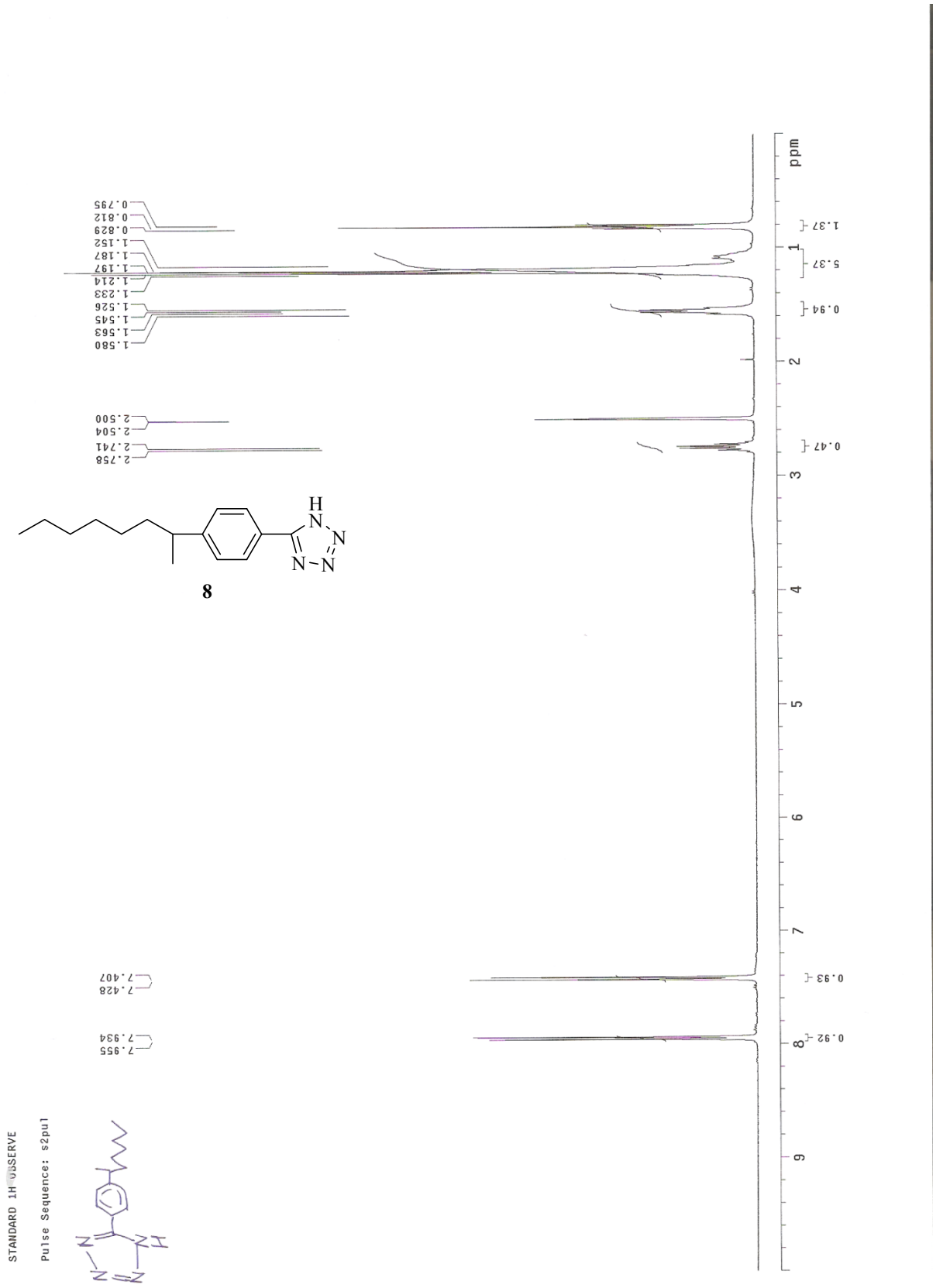

8

Supporting Figure S17. ^{13}C NMR Spectrum of **8**

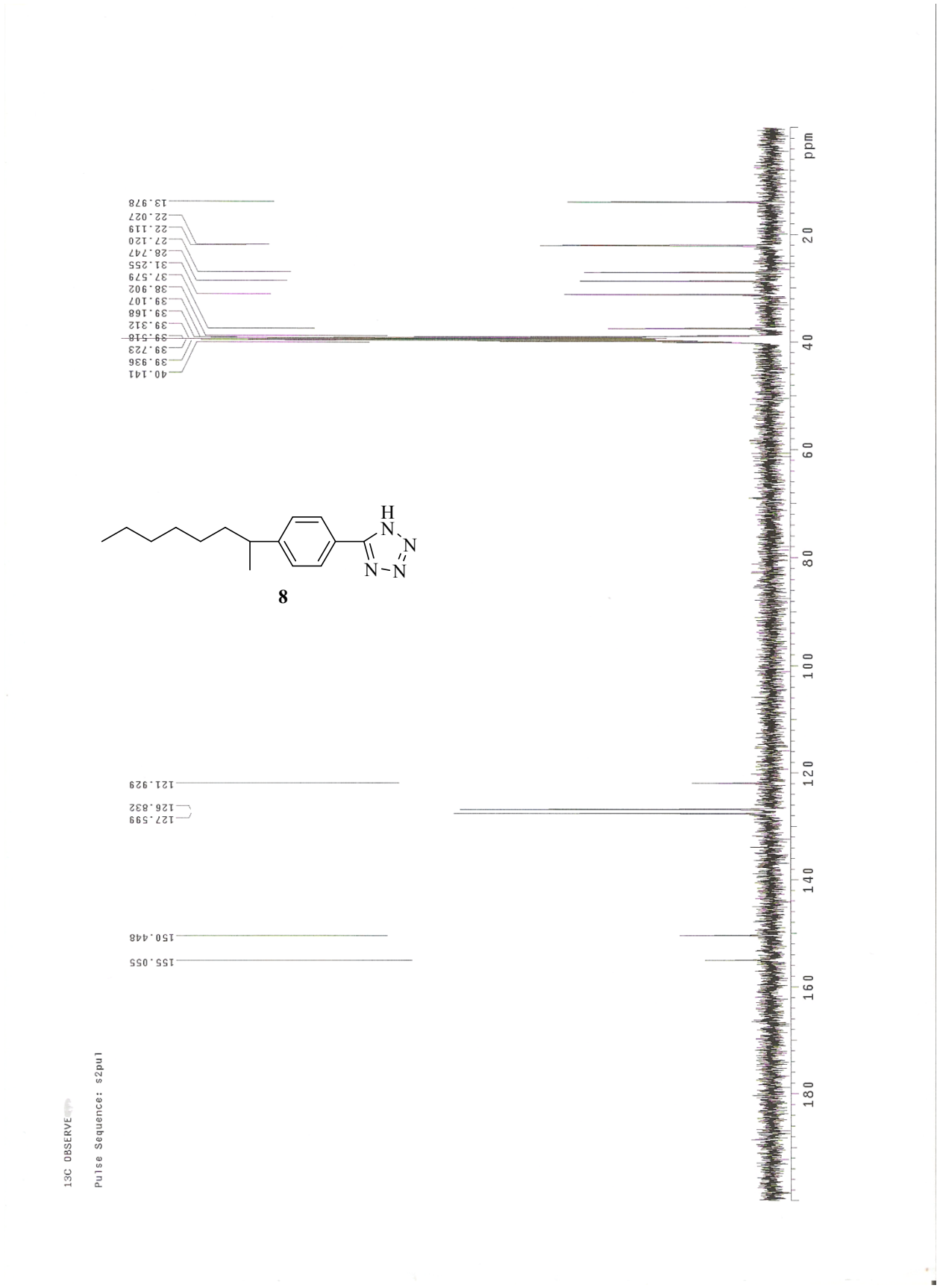

8

Supporting Figure S18. ^{1}H NMR Spectrum of **NOXD**

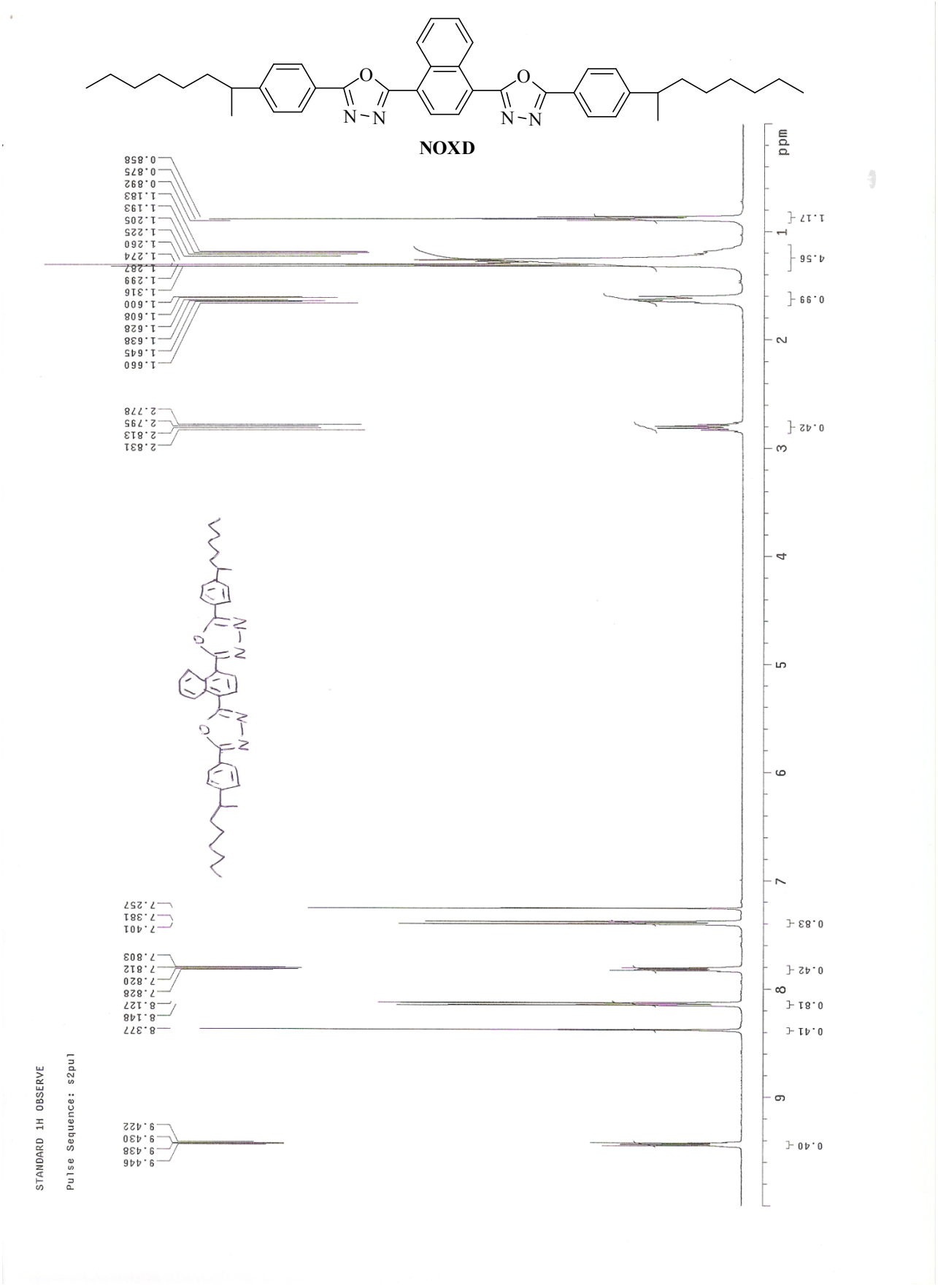

Supporting Figure S19. ^{13}C NMR Spectrum of **NOXD**

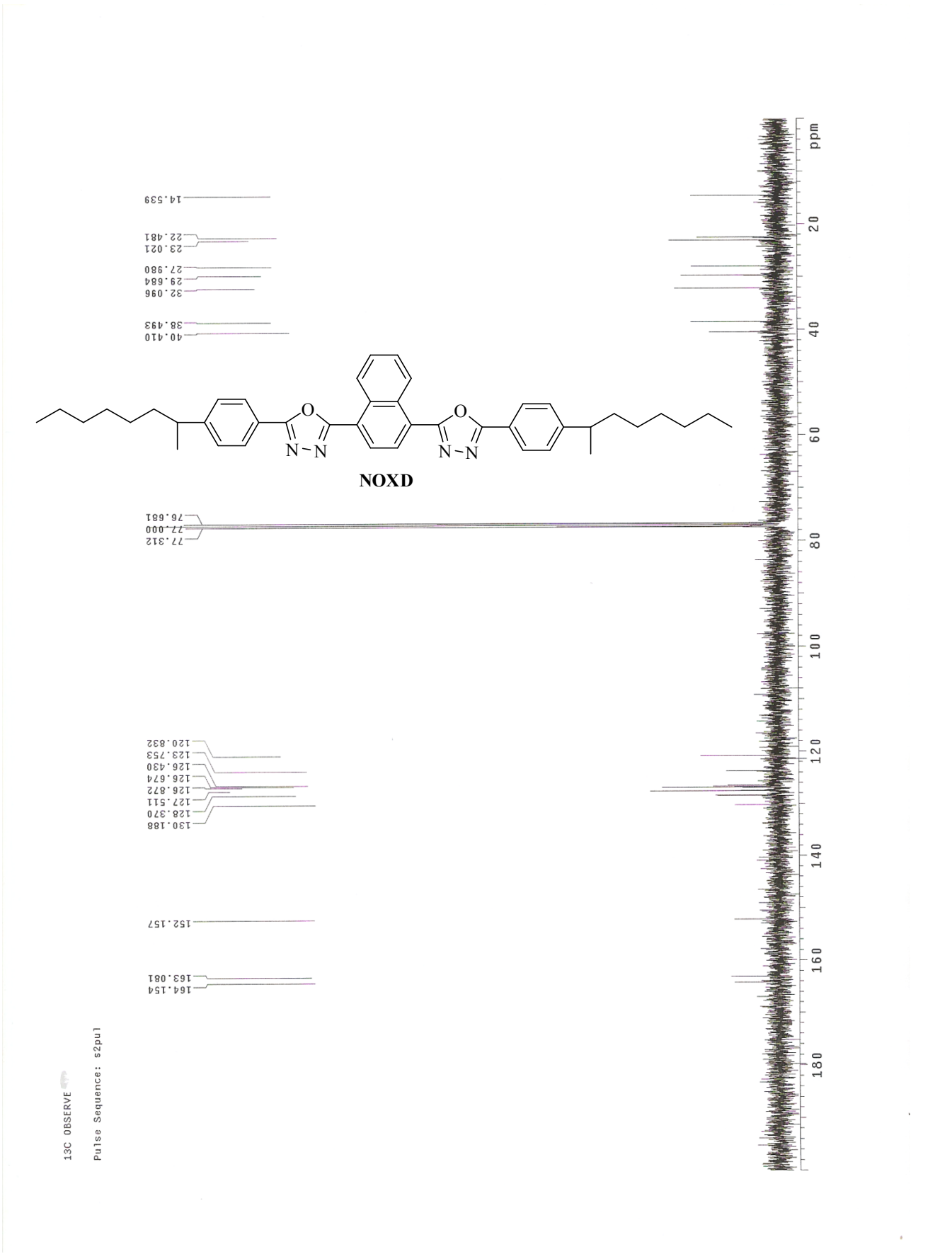

Supporting Figure S20. Theoretical UV-Vis spectral analysis of **NOXD**

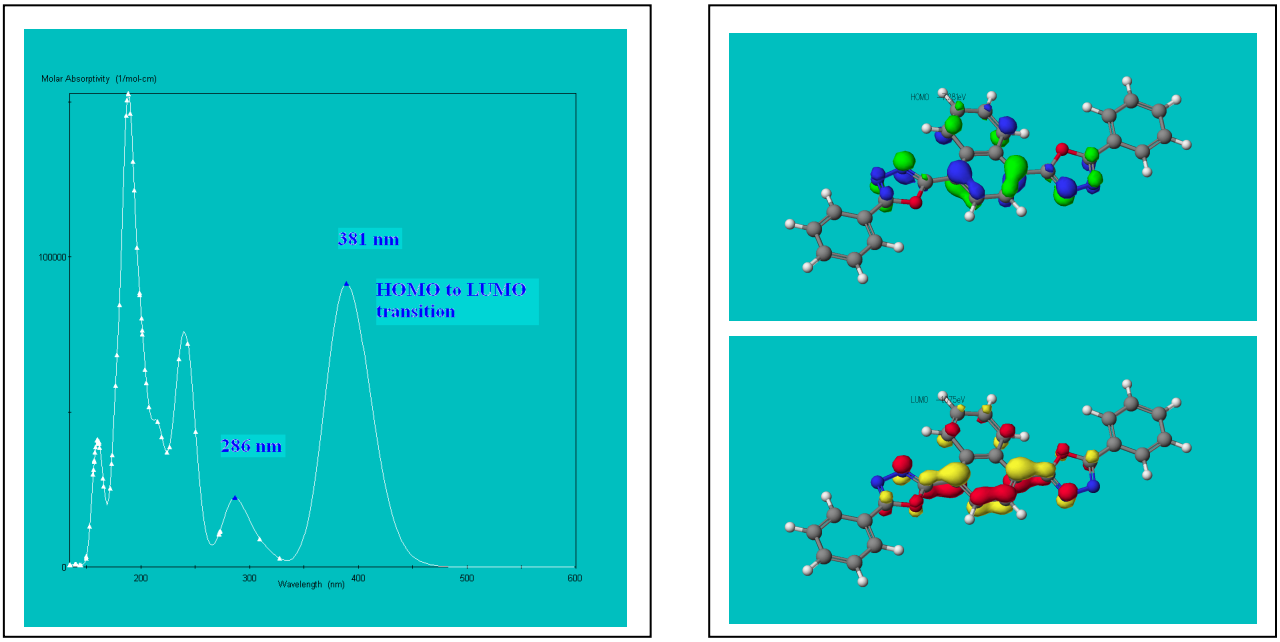

Theoretical UV-Vis spectral assignments are based on the molecular mechanics geometrical optimization and PM5/ZINDO calculations. The theoretical predictions are highly consistent with the experimental spectral data we obtained: The first transition at 360 nm is arising from HOMO/LUMO transition. The second band contains contributions from other 5 transitions.

Supporting Figure S21. Cyclic voltammograms of **NOXD** in TBAP/DMF (0.1M) under N_2 with a scan rate of 100 mV/s. A Glassy Carbon electrode was used as the working electrode versus a AgCl/Ag electrode as the reference electrode, and a Pt wire, as the counter electrode. The voltage was calibrated by using ferrocene as the internal standard.

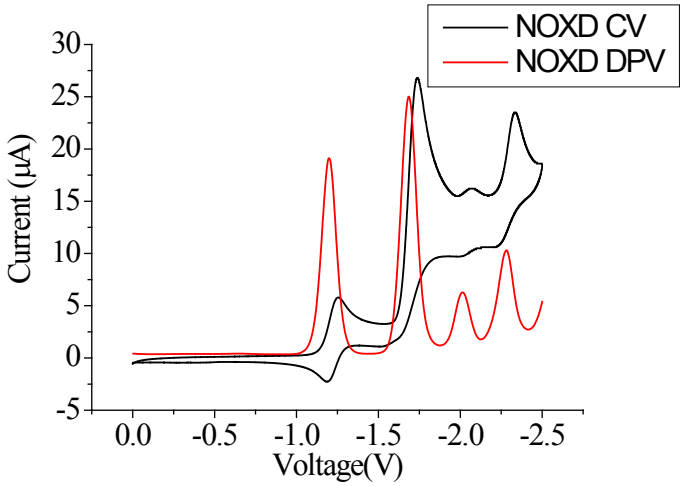

Supporting Figure S22. Cyclic voltammograms of PFT in TBAP/CH_2Cl_2 (0.1M) with a scan rate of 100 mV/s.

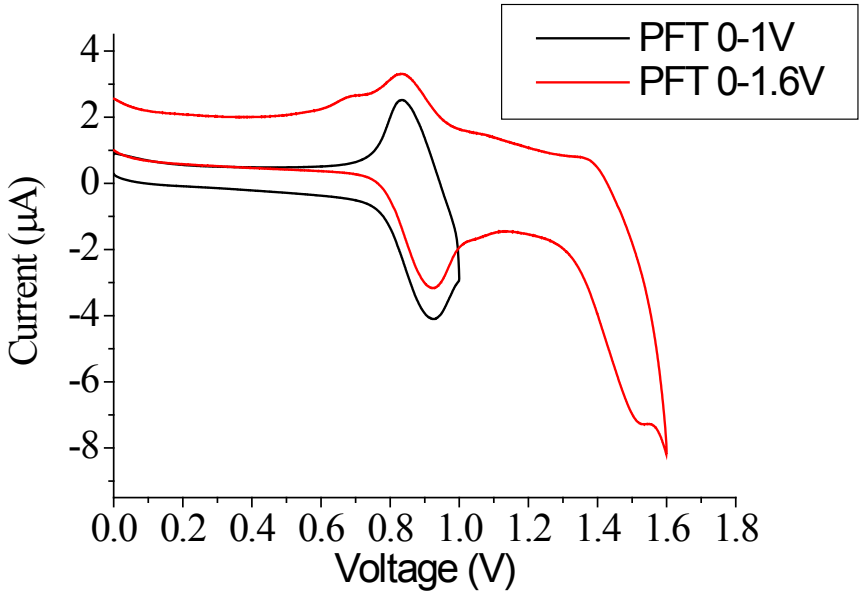

Supporting Figure S23. Time-resolved photoluminescence measurements of the **NOXD:PFT**.

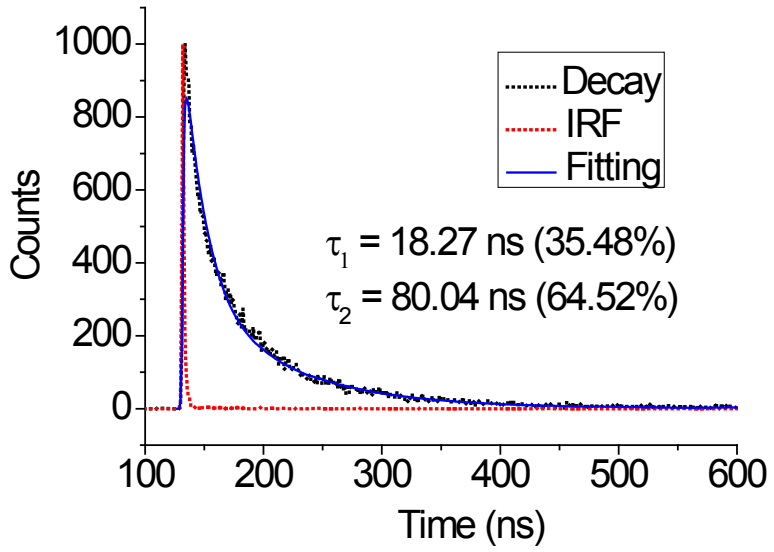

EXPERIMENTAL PROCEDURES

The fluorescence lifetime was detected using a time-correlated single photon counting (TCSPC) unit of an Edinburgh FLSP920 instrument. Samples were excited at 337 nm from a nitrogen pulsed flashlamp with 1 ns fwhm pulse duration transmitted through a Czerny-Turner design monochromator. Photomultiplier tube was employed as the detector. The instrument response function was profiled using a scatter solution and subsequently deconvoluted from the emission data to yield an undisturbed decay. Nonlinear least-squares fitting of the decay curves were performed with the Levenburg-Marquardt algorithm and implemented with the Edinburgh Instruments F900 software. The quality of the fits was judged by the χ^2 values and distribution of the residuals. The fitting curve based on two single-exponential decay components ($\tau_1 \sim 18.27$ ns, $\tau_2 \sim 80.04$ ns).